Concurrent and Independent Binding of Fcγ Receptors IIa and IIIb to Surface-Bound IgG

Tom E. Williams,* Shanmugam Nagarajan,† Periasamy Selvaraj,† and Cheng Zhu*

*George W. Woodruff School of Mechanical Engineering and Georgia Tech/Emory Department of Biomedical Engineering, Georgia Institute of Technology, Atlanta, Georgia 30332-0363 and †Department of Pathology and Laboratory Medicine, Emory University School of Medicine, Atlanta, Georgia 30322 USA

ABSTRACT Fc receptor–antibody interactions are key mechanisms through which antibody effector functions are mediated. Neutrophils coexpress two low-affinity Fcγ receptors, CD16b (FcγRIIIb) and CD32a (FcγRIIa), possessing overlapping ligand binding specificities but distinct membrane anchor and signaling capacities. Using K562 cell transfectants as a model, the kinetics of both separate and concurrent binding of CD16b and CD32a to surface-bound IgG ligands were studied. CD16b bound human IgG with 2–3 times higher affinity than did CD32a (A_cK_a = 4.1 and 1.6 $\times$ 10^{-7} μm^4, respectively) and both FcγRs had similar reverse kinetic rates (k_r = 0.5 and 0.4 s^{-1}, respectively). Because CD16b is expressed on neutrophils at a 4–5 times higher density than CD32a, our results suggest that CD16b plays the dominant role in binding of neutrophils to immobilized IgG. The question of possible cross-regulation of binding affinity between CD16b and CD32a was investigated using our multispecies concurrent binding model (Zhu and Williams, *Biophys. J.* 79:1850–1857, 2000). Because the model assumes independent binding (no cooperation among different species), the excellent agreement between the model predictions and the experimental data suggests that, when coexpressed on K562 cells, these two FcγRs do not interact in a manner that alters the kinetic rates of either molecule.

INTRODUCTION

Human neutrophils, which comprise over 70% of all circulating leukocytes, constitutively express two low-affinity FcγRs at resting state, FcγRIIa (CD32a) and FcγRIIIb (CD16b) (Salmon et al., 1996). Binding to antigen-complexed IgG brings about the cross-linking of FcγRs, which trigger a wide variety of immune responses. These may include clearance of immune complex, antibody-dependent cell-mediated cytotoxicity, phagocytosis, release of inflammatory mediators, and regulation of lymphocyte proliferation and differentiation (van de Winkel and Capel, 1996; Fridman and Sautes, 1997). As such, the knowledge of FcγR–IgG interactions is fundamental to the understanding of inflammatory processes and body defense by the immune system.

CD32a and CD16b^{NA2} are the subjects of the present study. CD32, a 40-kDa protein, is the most widely distributed Fc receptor. It has an extracellular portion that consists of two Ig-like domains, a single-span polypeptide transmembrane segment, and a cytoplasmic domain that contains an immunoreceptor tyrosine-based activator motif. Two allotypes of CD32a are known and are characterized by either an arginine or histidine residue at amino acid position 131. About 50% of Caucasians and 40% of Asians heterozygously express both CD32a^{R131} and CD32a^{H131} (Rascu et al., 1997), a mix we collectively denote herein as CD32a$^{R/H131}$. CD16b, a 50–70-kDa glycoprotein, is the predominant Fc receptor in blood, and is only expressed on neutrophils. It has an ectodomain that shares a high degree of homology with CD32a. However, it lacks the transmembrane and cytoplasmic domains, and anchors to the cell surface by means of a glycosyl phosphatidylinositol moiety. Like CD32a, two allotypes of CD16b exist, denoted NA1 and NA2 (Edberg et al., 1989; Ravetch and Perussia, 1989; Scallon et al., 1989; Selvaraj et al., 1988, 1989) (Fig. 1).

The biological significance of coexpressing two FcγRs with overlapping ligand-binding specificity (but distinct membrane anchors and signaling capacities) is not fully understood. It has been suggested that CD16b and CD32a may have distinct functional roles, can be differentially regulated, and may cooperatively interact (Selvaraj et al., 1989; Edberg and Kimberly, 1994; Edberg et al., 1998). The density of CD16b expressed on neutrophils is 4–5 times higher than that of CD32a (135,000 vs. 31,000 mol/cell) (Selvaraj et al., 1988). In addition, CD16b binds immobilized IgG with a nearly threefold higher affinity than CD32a (this study). Thus, CD16b should be the primary FcγR that neutrophils use to engage in initial binding. These two FcγRs also differ in their signaling capacities. Cross-linking of neutrophil CD32a induces degranulation, Ca^{2+} mobilization, erythrocyte cytotoxicity, tumor cell cytotoxicity, respiratory burst, and phagocytosis. Under similar conditions, neutrophil CD16b is capable of delivering signals for the former three but not for the latter three FcγR-dependent functions (Perussia et al., 1983; Shen et al., 1987; Lanier et al., 1988; Fanger et al., 1989; Selvaraj et al., 1989; Huizinga et al., 1990; Kimberly et al., 1990; Naziruddin et al., 1992). These data show that CD32a is a more potent trigger mol-

Received for publication 27 September 1999 and in final form 6 July 2000.

Address reprint requests to Cheng Zhu, George W. Woodruff School of Mechanical Engineering, and Georgia Tech/Emory Department of Biomedical Engineering, Georgia Institute of Technology, Atlanta, GA 30332-0363. Tel.: 404-894-3269; Fax: 404-385-1397; E-mail: cheng.zhu@me.gatech.edu.

0006-3495/00/10/1867/09 $2.00

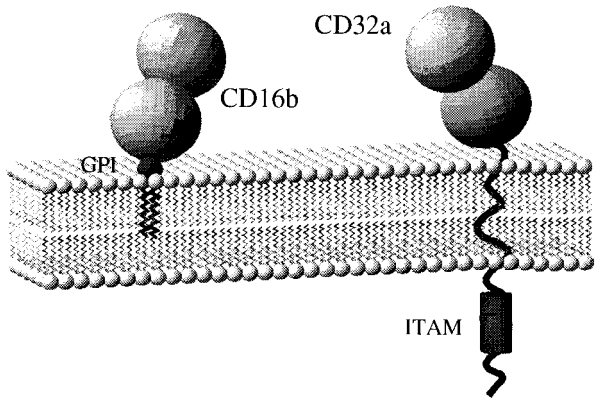

FIGURE 1 Schematics of the glycosyl phosphatidylinositol (*GPI*)-anchored CD16b and the polypeptide-anchored CD32a molecules. The Ig-like domains are depicted as globules. The immunoreceptor tyrosine-based activator motif (*ITAM*) is also shown.

ecule than CD16b. It has been suggested that CD16b signaling may be cross-regulated by CD32a (Naziruddin et al., 1992; Edberg and Kimberly, 1994), but it is not known whether such interaction includes affinity modulations. The affinity state of neutrophil CD32a has been found to be upregulated by activation of neutrophils with a bacterial chemotactic peptide, fMLP. With the same treatment, however, CD16b is shed from the neutrophil surface (Nagarajan et al., 2000).

To examine whether the suggested cross-regulation of CD16b and CD32a occurs at the level of affinity modulation, in the present paper, we measured the kinetics and equilibrium binding of these two FcγRs using the micropipette binding frequency assay. The experiments used, as a model for neutrophils, a human erythroleukemia K562 cell line that natively expressed CD32a$^{R/H131}$ (Warmerdam et al., 1990) and was transfected to express CD16b^{NA2} at a ratio similar to that on neutrophils. Micropipette adhesion frequency experiments were performed, using human red blood cells (RBC) to present membrane-bound IgG ligands. To examine the two FcγRs separately, adhesion-blocking monoclonal antibodies (mAb) were used to sequentially inhibit the function of each unwanted receptor. Experiments were also performed in the absence of any blocking mAb to allow concurrent binding of both FcγRs to cell-bound IgG. The single-receptor binding data obtained in the blocking experiments were analyzed using the single-species adhesion model of Chesla et al. (1998). The estimated kinetic rate and binding affinity constants were then used as input to a multiple-species model (Zhu and Williams, 2000) to predict the concurrent binding of CD16b and CD32a in the nonblocked experiments. Just as with the multiple ligand cases presented in Williams et al. (2000), the multiple receptor data corresponded quite well with the 95% prediction intervals generated in this manner, providing additional support for the multispecies theory.

One of the underpinning assumptions of these adhesion models is that the formation (and dissociation) of each discrete bond is independent of any others. This precludes competition or adhesion-dependent affinity regulation between or among receptor and ligand species. Therefore, the excellent agreement between the prediction and the data suggests that, when CD16b^{NA2} and CD32a$^{R/H131}$ are coexpressed on K562 cells, the binding of a soluble blocking mAb or immobilized ligand to either receptor does not alter the kinetic rates of the other.

MATERIALS AND METHODS

Antibodies and cells

The monoclonal antibodies CLBFcgran1 (anti-CD16, mIgG2a), 3G8 (anti-CD16, mIgG1), IV.3 (anti-CD32, mIgG2b), TS2/9 (anti-CD58, mIgG1), and X63 (no known human antigen, mIgG1) were purified in-house from hybridoma culture supernatant by protein G affinity chromatography, as previously described (Selvaraj et al., 1988; Nagarajan et al. 2000). Fab fragments of CLBFcgran1 and IV.3 were cleaved by Lampire (Pipersville, PA). Murine mAb GG7 (anti-human IgG Fc) was obtained as ascites fluid from Sigma Chemical Company (St. Louis, MO). Other negative control murine mAbs with no known human antigens obtained from Sigma included UPC-10 (mIgG2a) and MOPC-141 (mIgG2b). The goat anti-mouse FITC-conjugated polyclonal antibody used for flow cytometry was also from Sigma and the total serum human IgG used as ligand for FcγRs was from Lampire.

The human erythroleukemia K562 cell line was from American Type Cell Culture (Rockville, MD). Transfectant K562 cells expressing CD16b^{NA2} were established by cotransfecting a pCDM8 vector containing the CD16b^{NA2} gene and a pSV vector containing a hygromycin gene. We have previously described a similar transfection with these genes into CHO cells (Nagarajan et al., 1995). Transfected cells were selected with 400 μg/ml hygromycin and maintained in RPMI 1640 media plus 10% FCS containing 200 μg/ml of hygromycin. The cell density in the culture was no higher than 5×10^5 cells/ml. Human RBCs were isolated from whole blood of normal healthy volunteers as described in Williams et al. (2000).

Chromium chloride coupling of IgG and determination of receptor and ligand densities

Human IgG (or IgG-free ovalbumin) was covalently coupled to the membranes of RBCs by means of a chromium chloride ($CrCl_3$) method (Kofler and Wick, 1977). Site densities of IgG on RBC surfaces were determined by quantitative indirect fluorescent immunoassay using CD58 expression as a reference. The expression of CD16b and CD32a on the transfected and nontransfected K562 cells was observed by flow cytometry to be stable under the culture conditions described earlier. Receptor site density was quantified by radioimmunoassay using ^{125}I-labeled Fab fragments against CD16 (CLBFcgran1) or CD32 (IV.3). Detailed procedures have been presented in Williams et al. (2000).

Micropipette binding-frequency assay

Healthy cells of similar, roughly average size were individually selected by micropipette for subsequent adhesion testing. The micropipette system and the binding-frequency assay have been described in detail previously (Chesla et al., 1998, also see Williams et al., 2000). In essence, the assay measures an adhesive chemical reaction mechanically, because the products of the reaction are bonds that physically link the ligand-presenting

RBC to the receptor-expressing K562 cell. A micropipette-aspirated RBC picoforce transducer is used to detect *adhesion*, not to measure adhesion *force*; the quantity of interest is adhesion probability, not adhesion strength. Adhesion probability is estimated from the frequency of adhesion events observed in a large number of repeated cell–cell contacts, controlled by micromanipulation. The kinetic rate and equilibrium affinity constants are extracted from the dependence of the adhesion probability on contact duration, along with the independently measured receptor and ligand densities.

For the parameter evaluation to work well, the receptor and ligand densities should be adjusted in accordance with the binding affinity such that the adhesion probability data are in the mid ranges. A high-affinity interaction that results in an adhesion probability of nearly 100% cannot be easily distinguished from an interaction of twice that affinity. Similarly, it is difficult to distinguish a low-affinity interaction that yields a low adhesion probability (e.g., $<10\%$) from one of half that affinity. Both data before and including steady state are important, because the equilibrium binding affinity is related to the maximum (steady-state) adhesion frequency and the reverse kinetic rate is related to the time required to achieve a half-maximal adhesion frequency. It is therefore difficult to apply the assay to slow reactions, because the requirement for measuring adhesion probability through repeated contacts becomes prohibitive when each contact duration is long. Finally, the molecular system should be such that no appreciable depletion (or enhancement) of functionality occurs during the repeated tests. Gradual declines (or inclines) in adhesion frequency during the course of repeated tests can render error in the adhesion probability estimates. All of the above requirements were satisfied in our system of CD16b-transfected K562 cells and IgG-coated RBCs.

Data analysis

Kinetic rate and equilibrium affinity constants were extracted from the binding frequency data by iteratively reweighted nonlinear regression to the concurrent binding model (see Eq. 2) using the Levenberg–Marquardt algorithm (Wolfram Research, 1996). After analysis of the blocked data, prediction intervals (with 95% confidence levels) were computed for the expected mean response of the nonblocked experiments, assuming the validity of the concurrent binding model. Details of the weighting method and the prediction interval calculation are presented in Williams et al. (2000). Briefly, the micropipette data exhibit heteroscedasticity, or heterogeneity of variance, that needs to be corrected to obtain appropriate best-fit parameters, their standard errors, and prediction intervals. The reciprocal of the estimated variance was used as a weighting function in the nonlinear regression problem. A model was constructed for the variance of the adhesion probability based on its dependence on the variation in the receptor and ligand densities in the cell population. Determination of weights that best equalized the variance across the entire range of response required iteration. Once the single-species (blocked), iteratively reweighted, nonlinear least-squares problem was iterated to convergence, the regression parameter vector and the asymptotic covariance matrix were used to calculate the prediction intervals for the mean response under dual-species (nonblocked) conditions, following standard procedures (e.g., see Jennrich, 1995, Chapter 8).

RESULTS

CD16b is the dominant Fcγ receptor on CD16b-transfected K562 cells

As shown in Fig. 2, nontransfected K562 cells expressed CD32a but not CD16b, whereas the transfected cells expressed both CD16b and CD32a. The expression levels,

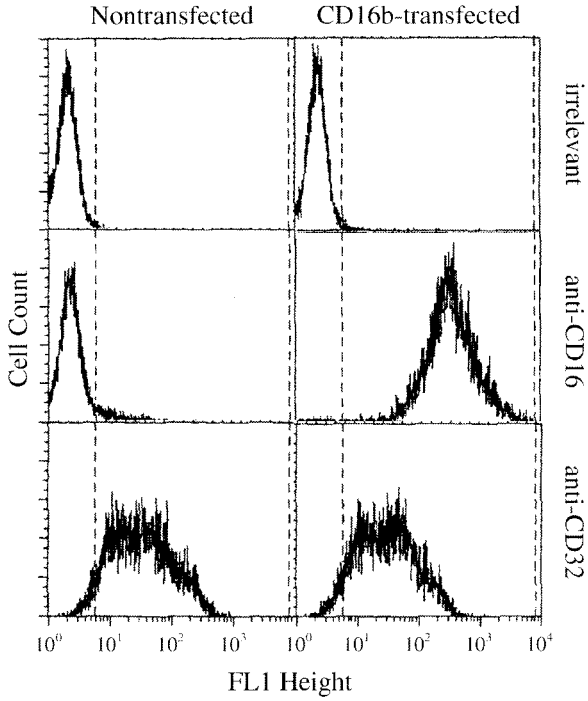

FIGURE 2 Fluorescence histogram of nontransfected (*left column*) and $CD16b^{NA2}$-transfected (*right column*) K562 cells. Cells were stained for flow cytometry using either anti-CD16 (3G8, *middle row*), anti-CD32 (IV.3, *bottom row*), or an irrelevant (X63, *top row*) murine mAb. The secondary antibody was a FITC-conjugated goat anti-mouse IgG polyclonal Ab.

quantified by radioimmunoassay, were 1.9×10^6 CD16b and 0.5×10^6 CD32a per K562 cell. To calculate expression density, the mean surface area of the K562 cells was determined from digital video micrography of over 100 healthy cells, yielding a mean apparent surface area of $584 \pm 13\ \mu m^2$ SEM. The derived site densities were 3250 CD16b and 860 CD32a per μm^2. Along with IgG coating densities of 35–650 per μm^2, this provided an excess of available receptors and ligands relative to the anticipated number of bonds in the contact area, ensuring that the effects of competition would be negligible (Zhu and Williams, 2000).

Adhesion of K562 transfectants to IgG-coated RBCs was due to specific FcγR binding

The single-species binding model used in previous studies (Piper et al., 1998; Chesla et al., 1998) has been extended to include multispecies concurrent binding in Zhu and Williams (2000). When binding is independent, the probability of specific adhesion during a cell–cell contact takes the form

$$P_S = 1 - \exp\left[-\sum_{i=1}^{N}\langle n_i\rangle\right], \tag{1a}$$

where

$$\langle n_i \rangle = m_{r_i} m_\ell A_c K_{ai}[1 - \exp(-k_{ri}t)] \qquad (1b)$$

is the average number of bonds formed by either CD16b (denoted by subscript 1) or CD32a (denoted by subscript 2). m_r and m_ℓ are the respective surface densities of the receptors and ligands. K_a is the two dimensional (2D) equilibrium binding affinity, and k_r is the reverse rate. t and A_c are contact duration and area, respectively. Retaining only a single $\langle n_i \rangle$ term in Eq. 1 reduces it to the single-species model (Chesla et al., 1998). These adhesion probability models are readily applied to dual-micropipette assays.

Micropipette binding-frequency assays were performed using IgG-coated RBCs to repeatedly contact CD16b-transfected K562 cells preincubated with either adhesion-blocking mAbs against one or both of the FcγRs or isotype-matched irrelevant control mAb (all at 10 μg/ml concentration), or without any antibody. The adhesion frequency versus contact time data was fit to the single-species version of Eq. 1 to extract an $m_r A_c K_a$ value for each condition. When only a single-receptor species was present (Fig. 3 *A*), this parameter was the equilibrium average number of bonds per unit density of IgG ligand. (Note that these bond averages are over all contacts, not just those that resulted in adhesion.) When both FcγRs were present (Fig. 3 *B*), the single-species model yielded the homogenized receptor approximation to the dual-receptor binding (Zhu and Williams, 2000). The fitted parameter $\overline{m_r A_c K_a}$ therefore approximated the equilibrium average number of total bonds per unit density of IgG ligand, $m_{r1} A_c K_{a1}$. The results in Fig. 3 show that the $m_r A_c K_a$ (or $\overline{m_r A_c K_a}$) value was reduced by treatment of anti-CD16 (CLBFcgran1, mIgG2a) and anti-CD32 (IV.3, mIgG2b) mAbs but not by treatment of irrelevant mAbs, regardless of isotype. Blocking with whole Ab produced comparable results to those produced with cleaved Fab fragments. These data demonstrate the specificity of the adhesion probabilities measured in the micropipette experiments. It is also evident that, on average, CD16b contributed much more to the formation of FcγR-IgG bonds in this system than did CD32a when the other receptor was blocked by mAb. This suggests that, relative to CD16b, CD32a may have a lower 2D affinity for IgG in addition to the lower expression level discussed earlier. This suggestion was confirmed in subsequent analysis, detailed later.

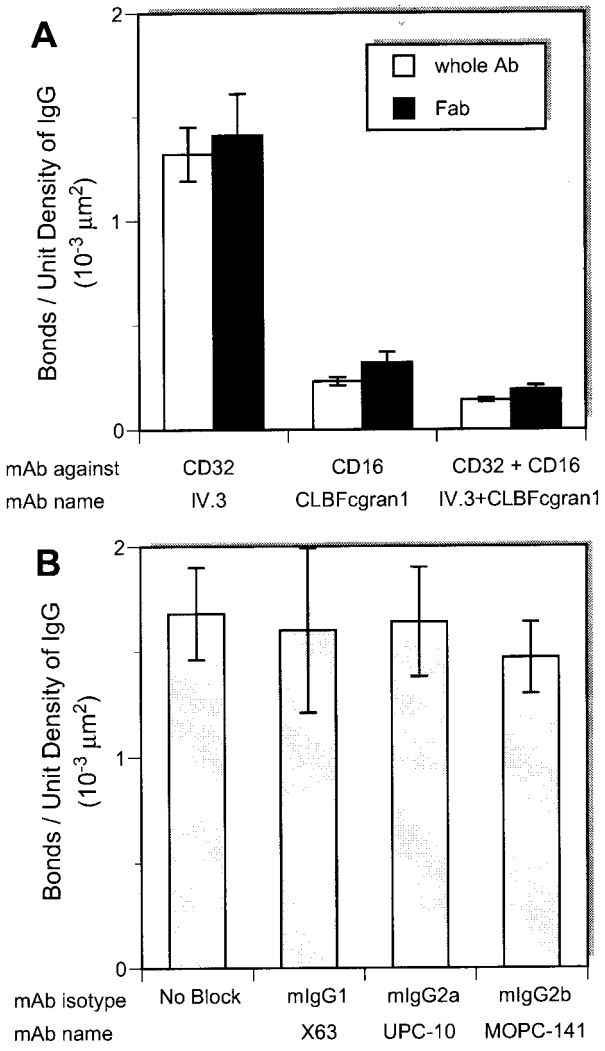

FIGURE 3 (*A*) Anti-FcγR mAb blocking and (*B*) isotype-matched irrelevant mAb control experiments. Soluble Fab and whole forms of anti-CD16 (CLBFcgran1, mIgG2a) and anti-CD32 (IV.3, mIgG2b) mAbs, as well as whole irrelevant mAbs of various isotypes, were tested alone or in combination for their ability to block binding of CD16b-transfected K562 cells to IgG-coated RBCs in the micropipette assay. Adhesion frequency data so obtained was analyzed by the single-species version of Eq. 1, and the resulting values for the mean number of bonds present at equilibrium per unit density of IgG are shown. $N = 5$ cell pairs, each at a different contact time, with 100 contact cycles each. Ligand densities were 35–650 IgG/μm^2. Error bars represent standard errors on the estimated means.

Receptor blocking experiments follow the prediction of the single-species model

Data from all receptor-blocking experiments are shown in Fig. 4. To increase the reliability of the estimated binding parameters and the power of statistical inference in the prediction interval calculation, two preparations of IgG-coated RBCs (m_ℓ = 580 and 650 IgG/μm^2) were used for each blocking condition. CLBFcgran1 (anti-CD16 mAb) blocked most of the binding by itself (Fig. 4 *B*), though IV.3 (anti-CD32 mAb) had a clearly discernible effect when added alone (cf. Fig. 4 *A* with Fig. 6, *A* and *B*) or together with CLBFcgran1 (Fig. 4 *C*). When the RBCs were coated with IgG-free ovalbumin instead of IgG, the nonspecific binding to the transfectant K562 cells was similar to that of the double-blocking experiment with both IV.3 and CLB-Fcgran1 present (Fig. 4 *D*).

By adding an empirical expression describing the proba-

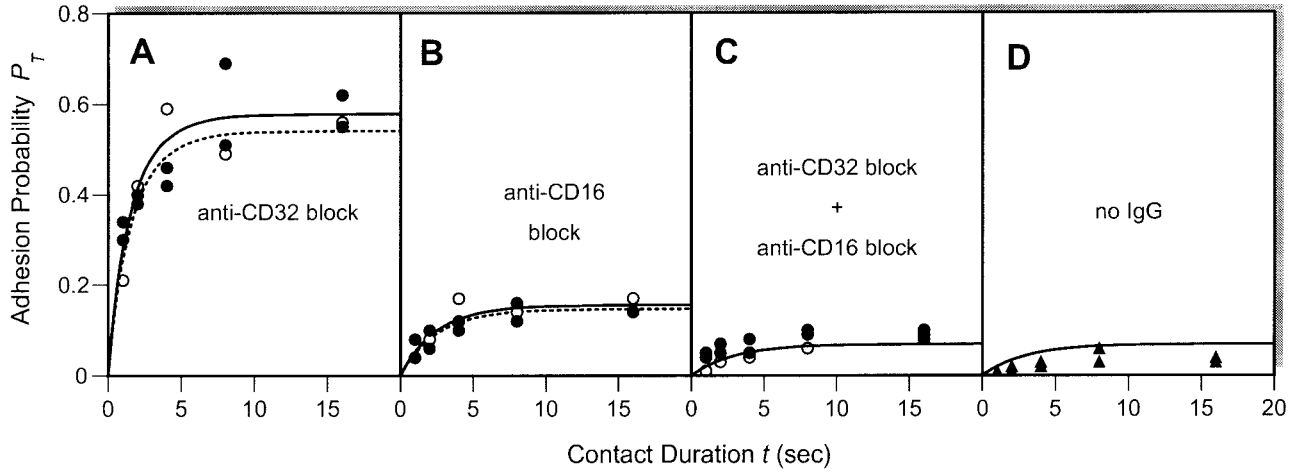

FIGURE 4 Binding curves from receptor blocking experiments. (*A–C*) One or both of the Fcγ receptors were blocked from participation in binding to human IgG-coated RBCs by pre-incubating the transfectant K562 cells with the indicated antibody or antibodies (10 μg/ml, 30 min) and conducting micropipette binding frequency assays in the continuous presence of the antibody or antibodies (2 μg/ml). (*D*) An additional experiment was performed with nonblocked transfectant K562 cells binding to IgG-free ovalbumin-coated RBCs. Each point represents total adhesion probability estimated from one cell pair with 100 contact cycles. Curves are derived from the best-fit kinetics parameters obtained from applying the concurrent binding model (Eq. 2) to all blocking data simultaneously, treating the data in (*A*) as CD16b only, (*B*) as CD32a only, and (*C* and *D*) as nonspecific binding. IgG site densities were 580 μm^{-2} (○, *dotted curves*) or 650 μm^{-2} (●, *solid curves*).

bility of nonspecific adhesion to the model for P_S given in Eq. 1, the following general model for the total probability of adhesion is obtained (Zhu and Williams, 2000):

$$P_T = 1 - \exp\left[-a(1 - e^{-bt}) - \sum_{i=1}^{N}\langle n_i\rangle(1 - \delta_i\beta_i)\right]. \qquad (2)$$

This can then be used to simultaneously fit both the nonspecific binding (characterized by parameters a and b) and the specific adhesions that are mediated by N (= 2 for the present case) species of receptor–ligand bonds. Here we have also provided an element to account for the presence of blocking agents. δ_i is the blocking score, and it is defined to be equal to 1 if the ith receptor species is blocked and 0 if it is not blocked. β_i is the blocking efficiency of the mAb against the ith receptor species.

For the purpose of model testing, we neglected any blocking inefficiency. A single set of binding constants was determined by fitting all blocking data shown, as well as the nonspecific data, to Eq. 2, assuming $\beta_i = 1$ (i.e., complete blocking) for both IV.3 and CLBFcgran1. The four binding parameters so determined are listed in Table 1 and form the basis for the curves shown in Fig. 4 (and the prediction intervals of Fig. 6, discussed below).

Blocking is nearly complete

If the inhibitory antibodies, at the concentrations used (10 μg/ml), were able to block all target receptors perfectly, then adding both antibodies would completely eliminate specific binding. The remaining binding would be entirely nonspecific and would therefore be independent of the ligand density used. Similarly, removal of the ligand by replacement with IgG-free ovalbumin would leave only nonspecific binding. Therefore, in the preceding section, the data in Fig. 4 *C* (no available receptors) and Fig. 4 *D* (no ligands) were treated as equivalent under the complete blocking assumption, and a single curve was generated to fit both sets. It is apparent, however, that the combined use of both blocking antibodies was still insufficient to inhibit all

TABLE 1 Summary of binding parameters for total human IgG

	A_cK_a (10^{-7} μm^4)		k_r (s^{-1})		
Data Set	$CD16b^{NA2}$	$CD32a^{R/H131}$	$CD16b^{NA2}$	$CD32a^{R/H131}$	$\bar{\beta}$
Blocking data only	3.7 ± 0.3	1.8 ± 0.4	0.50 ± 0.10	0.43 ± 0.24	(1)
All data, β fixed	3.9 ± 0.2	1.9 ± 0.1	0.49 ± 0.06	0.43 ± 0.21	(1)
All data, β free	4.1 ± 0.2	1.6 ± 0.4	0.50 ± 0.06	0.38 ± 0.18	0.94

N = 44 and 81 cell pairs (100 contact cycles each) for blocking and all data, respectively. An additional 10 cell pairs were used to characterize the nonspecific binding.
Values are mean ± SE.

specific binding, indicating that a detectable number of receptors were not blocked by the antibodies. Using Eq. 2, the mean blocking efficiency $\bar{\beta}$ was estimated during the fitting of the data to be 94% ± 3%. (The data would have to be exceptionally tight and numerous to allow separate determination of β_i for each antibody, so it was necessary to presume that the antibodies behaved similarly in this regard.) During the regression, this parameter was free to take on any value, so its best-fit level near unity was a good indication that the blocking efficiency was nearly perfect at the concentrations used.

Use of this slightly incomplete blocking efficiency value of 94% results in a small shift in the extracted parameters and the curves generated by them. Dual-block experiments are no longer expected to match the no IgG curves, and are also ligand-density dependent. Figure 5 illustrates the improvement of the fit for these conditions when incomplete blocking is accommodated. The curves in Fig. 4, *A* and *B*, are minimally shifted (not shown). Still, although this method does provide a reasonable blocking efficiency estimate, addition of another free parameter to the model under evaluation might compromise the rigor of the predictive test. For this reason, we chose to present the blocking-data fits (Fig. 4) and the prediction intervals based on these fits (Fig. 6) without use of the blocking-efficiency concept. However, this effect is subsequently explored when final binding parameter estimates are made.

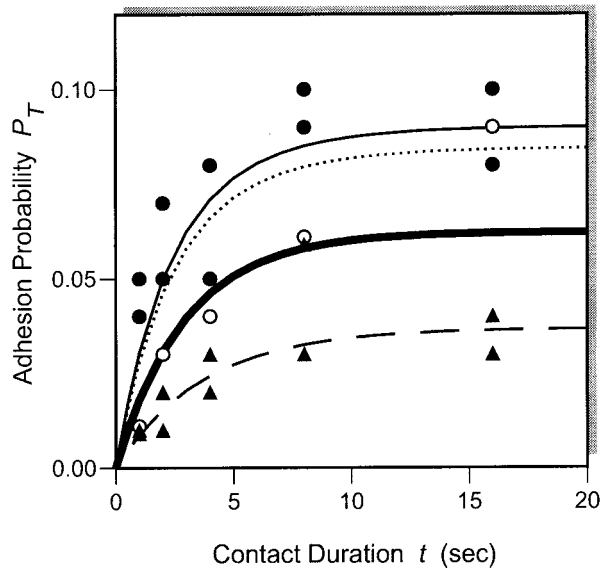

FIGURE 5 Effects of blocking efficiency. If antibody blocking was complete, the "no receptor" cases (Fig. 4 *C*) and the "no ligand" case (Fig. 4 *D*) would be the same. When antibody blocking efficiency was estimated from the data, the mean blocking efficiency $\bar{\beta}$ was 94% and the single solution in Fig. 4, *C* and *D* (shown here as the bold solid curve), became three separate ones. Here, the best fit responses of the 6% of residual receptors interacting with two coating densities of ligands, 580 IgG/μm^2 (○, *dotted curve*) and 650 IgG/μm^2 (●, *thin solid curve*), were distinctly higher than that of the nonspecific "no ligand" case (▲, *dashed curve*).

Prediction of nonblocked response is accurate

To provide a rigorous test of the concurrent binding model (Zhu and Williams, 2000), a large number of micropipette experiments were conducted under nonblocking conditions using CD16b-transfected K562 cells against IgG-coated RBCs at levels ranging from 650 down to 35 molecules of IgG per μm^2. The kinetic-rate and binding-affinity constants for CD16b^{NA2} and CD32a$^{R/H131}$, derived from the blocking data alone as described above ($\beta \equiv 1$), were used to generate prediction intervals for the mean response to nonblocked binding, using Eq. 2 with all δ_i set to zero. Adhesion frequency data and prediction intervals for each ligand-density level are shown in Fig. 6. The excellent correspondence illustrates the strong predictive ability of the model when applied to micropipette experiments. It also suggests that the simplifying assumptions underlying the concurrent binding model, most noticeably that of independent binding, are valid for the system tested.

Best estimates of the binding parameters

Binding curves from both blocked and nonblocked conditions were simultaneously fit to the concurrent binding model (Eq. 2), with either a fixed $\bar{\beta}$ value of unity or allowing it to vary as an additional freely-adjustable fitting parameter. The resulting kinetic rate and binding affinity constants are presented in Table 1, which show excellent agreement with those estimated from fitting the blocked data alone, imparting more confidence in the concurrent binding model.

The data presented in Figs. 4 and 6 were collected from a large number of experiments performed over the course of several months using different preparations of cells and reagents. As such, the standard errors generated by curve-fitting the entire data set should include not only intra-experimental variations of individual data points (e.g., cell-to-cell variability in the same sample) but also inter-experimental variations of individual subsets of data (e.g., variability among different preparations). This is in contrast to standard errors generated by regressing data from only a single experiment, which, in general, only account for intra-experimental variations, and hence are often much smaller than the standard errors calculated from multiple parameter values, each of which is estimated from an individually repeated experiment. Thus, the small standard errors shown in Table 1 are indicative of both data quality and model validity.

Although the reverse kinetic rates of the two receptors were very similar in these data, the equilibrium binding affinity of CD16b^{NA2} was greater than the affinity of CD32a$^{R/H131}$ by two- to threefold. This further confirms that CD16b is the dominant player in the FcγR–IgG-mediated adhesion in the transfectant K652 cells.

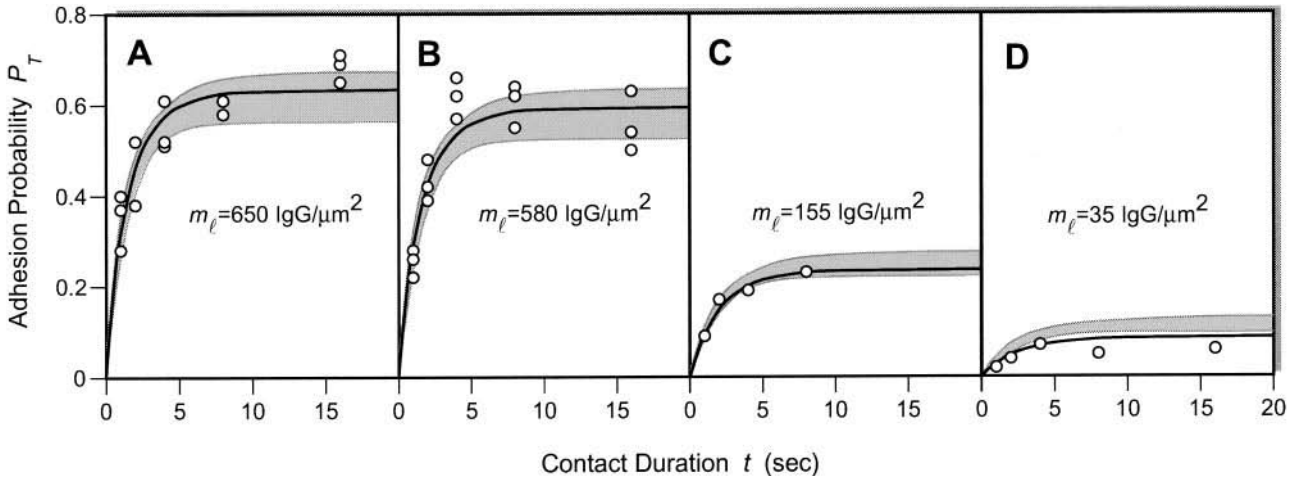

FIGURE 6 Nonblocked binding curves and prediction intervals. The adhesion of CD16b-transfected K562 cells was assayed against RBCs coated at ligand densities of (*A*) 650, (*B*) 580, (*C*) 155, and (*D*) 35 molecules of IgG per μm^2. Each point (○) represents a single cell pair with 100 contact cycles each. The solid lines were produced from the best-fit binding parameters extracted from the entire nonblocked data set. The 95% prediction intervals for the mean response (*shaded regions*), computed from blocking data alone, correspond well with the nonblocked best-fit curves.

DISCUSSION

A major goal of the present work was to quantify the kinetics of FcγR–IgG interactions. Like on neutrophils, the CD16b on our K562 transfectants outnumbered the CD32a by a factor of at least three. Possessing a substantially higher 2D affinity for IgG as well, CD16b played the dominant role in Fc-mediated adhesion. The kinetic rate and binding affinity constants of CD32a for surface-bound ligand (i.e., the so-called 2D binding parameters) have not been determined previously. These parameters were measured in the present study using the micropipette binding frequency assay. As with the CD16b^{NA2}–hIgG2 interaction described in Williams et al. (2000), the affinity of CD32a$^{R/H131}$–hIgG binding is quite low. Both represent the weakest receptor–ligand interactions for which 2D kinetic rates have ever been successfully measured.

The special case of two receptor species binding the same ligand species was examined to further test the validity of concurrent binding model developed in Zhu and Williams (2000). As in the case of two ligand species binding the same receptor species (Williams et al., 2000), the approach was to separate the data into two sets, using the results from one set to predict the results from the other set. In this case, results from sequential or simultaneous blocking of the two FcγRs coexpressed on CD16b-transfected K562 cells were used to predict results from various nonblocked conditions. Just as with the dual-ligand case, the experimental data matched the prediction intervals extremely well, providing substantial support for the concurrent binding model.

For purposes of comparing the association of two receptors to a common ligand, the human IgG was treated as a single uniform species. Total serum IgG consists of four isotypes with differing proportions and binding parameters for each FcγR. Neutrophils encounter mixtures of all isotypes, and, because it was not the objective of this work to examine isotype-dependent behavior, treating the total serum IgG as a homogeneous ligand provided a convenient simplification (Zhu and Williams, 2000).

In the dual-ligand case examined in Williams et al. (2000), the single-ligand binding was controlled by simply not coating the unwanted ligand species onto the RBCs. By comparison, in the present dual-receptor case the single-receptor binding was achieved by using an adhesion-blocking mAb to inhibit the function of the unwanted receptor. This represents a case of competitive binding between a soluble mAb and a cell-bound ligand for the same cell surface receptor. In a recent paper (Li et al., 1999), we described a model for such competitive inhibition except that, in the previous work, only a single receptor species was present on the cell surface. A straightforward extension of the model of Li et al. (1999) along the lines of reasoning as in Zhu and Williams (2000) would allow it to be applicable to the present case. Indeed, the effect of competition by the soluble mAb is fully described by the simple concept of blocking efficiency used in Eq. 2. Comparing Eq. 2 to the model of Li et al. (1999) yields the relation,

$$1 - \beta = \frac{1}{1 + cK_{a,3D}}, \tag{3}$$

where c is the volume concentration of the blocking mAb, and $K_{a,3D}$ is the three-dimensional (3D) binding affinity of the fluid-phase mAb for the cell surface antigen (i.e., FcγR). In fact, the nearly complete blocking efficiency ($\bar{\beta} = 94 \pm 3\%$) by specific antibodies is predicted by Eq. 3. For example, using $K_{a,3D} = 8.3 \times 10^7\ M^{-1}$ for CLBFcgran1 Fab–CD16b^{NA2} interaction (Chesla et al., 2000) and the concen-

tration ($c = 2 \times 10^{-7}$ M) of CLBFcgran1 Fab used in the blocking experiment, a β of 94.3% can be calculated from Eq. 3. Similarly, the control experiment with irrelevant antibodies is also a competition binding case. But the soluble competitors are of much lower $K_{a,3D}$ because here it is the Fc binding rather than Fab binding. The negligible blocking effect seen in Fig. 3 *B* is also predicted by Eq. 3, based on the low affinities for soluble IgG of the two FcγRs (e.g., $K_{a,3D} = 2$ and 3×10^4 M^{-1} for CD16b^{NA2} interacting with Fc of human and rabbit IgGs, Chesla et al., 2000) and the concentration of mIgG Fc used in the control experiment ($c = 6.7 \times 10^{-8}$ M).

Although CD32a is found on most leukocytes, it is constitutively coexpressed with CD16b only on neutrophils. Here there is evidence for cooperative interaction between these two FcγRs in the generation of calcium transients and the initiation of phagocytosis (Naziruddin et al. 1992; Edberg and Kimberly 1994; Edberg et al. 1998). Simultaneous cross-linking of both receptors, with either aggregated IgG or antireceptor antibody, generates a substantially stronger response than the sum of the responses to cross-linking of each receptor species separately. The assumptions of the concurrent binding model do not exclude synergy in these types of downstream effector functions. But they do preclude cooperation between the two receptor species that would result in synergy in ligand binding kinetics, or changes in receptor expressions. The high degree of correspondence between the nonblocked data and the prediction intervals derived from the blocked data suggests that the noncooperative assumption has adequately accounted for the binding kinetics of CD16b and CD32a when they are coexpressed on K562 cells. If saturation binding of one receptor by soluble antibody resulted in increased binding of the other receptor, the prediction intervals (based on such antibody treatment) for the untreated conditions would have been too high. This was not the case here.

Similarly, in the nonblocked experiment, both CD16b and CD32a were involved in the IgG-mediated adhesion. By comparison, in the blocked experiment, only one receptor was allowed to participate in the binding of cell-bound IgG ligands. Should IgG binding via both FcγRs have a synergetic effect, the prediction intervals would have been too low. Again, this was not seen here. A limited number of bonds likely formed during each period of contact, which itself endured for 16 s at most. However, the process was repeated many times as each cell pair was subjected to a series of 100 similar contacts, with cumulative contact periods of as much as 30 min. Adhesion frequency near the end of each series did not show any consistent difference from the frequency near the beginning (data not shown).

Additional evidence against the cross-FcγR affinity regulation hypothesis in our system comes from the agreement in the kinetic rates of CD16b^{NA2} when expressed on K562 cells (the present work) or Chinese hamster ovary (CHO) cells (Williams et al., 2000). CHO cells do not express CD32a, yet the CD16b kinetic rates obtained from that system ($A_cK_a = 3.3 \times 10^{-7}$ μm^4, $k_r = 0.56$ s^{-1}) were strikingly similar to their K562 cell counterparts ($A_cK_a = 4.1 \times 10^{-7}$ μm^4, $k_r = 0.50$ s^{-1}, see Table 1).

In this work, we have provided evidence that saturation binding of adhesion-blocking mAb to either CD16b or CD32a does not alter the ligand affinity of the other receptor when both are present on K562 cells. We similarly reject affinity-level cooperation in our model system when both receptors are allowed to concurrently bind to IgG. This is an important initial step in understanding cross-talk between these two molecules and in determining if and how the downstream interactions observed in neutrophils relate to their function as Fcγ adhesion receptors. Additional work is immediately suggested. It is likely that a portion of the mAb-bound receptors were also cross-linked when divalent whole mAb was used for adhesion blocking, so the similarity with the monovalent Fab blocking results (Fig. 3 *A*) implies that such intraspecies cross-linking did not stimulate any ligand affinity regulation. However, we have left unexplored the possible outcomes of interspecies cross-linking (i.e., CD16b–CD32a).

This work used CD16b-transfected K562 cells as a potential model for neutrophil FcγR functions. Our transfectant K562 is the only immortalized cell line that coexpresses both CD16b and CD32a. Furthermore, the relative expression levels of the two FcγRs are similar for both neutrophils and our transfectants. The availability of a perpetual supply of genetically uniform model cells offers clear advantages, and it is our hope that results derived from the K562 transfectants will provide a useful complement to direct neutrophil studies. Functional comparisons of both adhesion and signaling behavior in the two cells will be particularly critical. For example, if affinity cross-regulation can be demonstrated on the neutrophil, then the lack of such cross-talk in the K562 model would suggest the action of an intermediate agent, identification of which would be aided by its apparent absence on the K562 cells. The concurrent binding model and blocking approach presented in this report provide a good foundation for these studies. Such studies will help us to define the physiological significance of coexpressing different receptors with overlapping ligand specificity.

We would like to thank Dr. Ping Li for iodination of the CLBFcgran1 Fab mAb. This work was supported by National Science Foundation grants BCS 9210648 and BCS 9350370 and National Institutes of Health grant AI38282 (C.Z.), as well as National Institutes of Health grant AI30631 (P.S.). T.E.W. was also partially supported by National Institutes of Health Training grant GM08433.

REFERENCES

Chesla, S. E., P. Li, S. Nagarajan, P. Selvaraj, and C. Zhu. 2000. The membrane anchor influences ligand binding 2D kinetic rates and 3D affinity of FcγRIII (CD16). *J. Biol. Chem.* 275:10235–10246.

Chesla, S. E., P. Selvaraj, and C. Zhu. 1998. Measuring two-dimensional receptor-ligand binding kinetics by micropipette. *Biophys. J.* 75: 1553–1572.

Edberg, J. C., and R. P. Kimberly. 1994. Modulation of Fcγ and complement receptor function by the glycosyl-phosphatidylinositol-anchored form of FcγRIII. *J. Immunol.* 152:5826–5835.

Edberg, J. C., J. J. Moon, D. J. Chang, and R. P. Kimberly. 1998. Differential regulation of human neutrophil FcγRIIa (CD32) and FcγRIIIb (CD16)-induced Ca^{2+} transients. *J. Biol. Chem.* 273: 8071–8079.

Edberg, J. C., P. B. Redecha, J. E. Salmon, and R. P. Kimberly. 1989. Human FcγRIII (CD16). Isoforms with distinct allelic expression, extracellular domains, and membrane linkages on polymorphonuclear and natural killer cells. *J. Immunol.* 143:1642–1649.

Fanger, M. W., L. Shen, R. F. Graziano, and P. M. Guyre. 1989. Cytotoxicity mediated by human Fc receptors for IgG. *Immunol. Today.* 10: 92–99.

Fridman, W. H., and C. Sautes. 1997. Cell-mediated Effects of Immunoglobulins. R. G. Landes, Austin, TX.

Huizinga, T. W., K. M. Dolman, N. J. van der Linden, M. Kleijer, J. H. Nuijens, A. E. von dem Borne, and D. Roos. 1990. Phosphatidylinositol-linked FcRIII mediates exocytosis of neutrophil granule proteins, but does not mediate initiation of the respiratory burst. *J. Immunol.*144.: 1432–1437.

Jennrich, R. I. 1995. An Introduction to Computational Statistics: Regression Analysis. Prentice Hall, Englewood Cliffs, NJ.

Kimberly, R. P., J. W. Ahlstrom, M. E. Click, and J. C. Edberg. 1990. The glycosyl phosphatidylinositol-linked FcγRIII PMN mediates transmembrane signaling events distinct from FcγRII. *J. Exp. Med.* 171: 1239–1255.

Kofler, R., and G. Wick. 1977. Some methodologic aspects of the chromium chloride method for coupling antigen to erythrocytes. *J. Immunol. Methods.* 16:201–209.

Lanier, L. L., J. Ruitenberg, R. L. Bolhuis, J. Borst, J. H. Phillips, and R. Testi. 1988. Structural and serological heterogeneity of γ/δ T cell antigen receptor expression in thymus and peripheral blood. *Eur. J. Immunol.* 18:1985–1992.

Li, P., P. Selvaraj, and C. Zhu. 1999. Analysis of competition binding between soluble and membrane-bound ligands for cell surface receptors. *Biophys. J.* 77:3394–3406.

Nagarajan, S., S. Chesla, L. Cobern, P. Anderson, C. Zhu, and P. Selvaraj. 1995. Ligand binding and phagocytosis by CD16 (Fcγ receptor III) isoforms. Phagocytic signaling by associated ζ and γ subunits in Chinese hamster ovary cells. *J. Biol. Chem.* 270:25762–25770.

Nagarajan, S., K. Venkiteswaran, M. Anderson, U. Sayed, C. Zhu, and P. Selvaraj. 2000. Cell specific, activation dependent regulation of neutrophil CD32A ligand binding function. *Blood.* 95:1069–1077.

Naziruddin, B., B. F. Duffy, J. Tucker, and T. Mohanakumar. 1992. Evidence for cross-regulation of FcγRIIIB (CD16) receptor-mediated signaling by FcγRII (CD32) expressed on polymorphonuclear neutrophils. *J. Immunol.* 149:3702–3709.

Perussia, B., O. Acuto, C. Terhorst, J. Faust, R. Lazarus, V. Fanning, and G. Trinchieri. 1983. Human natural killer cells analyzed by B73.1, a monoclonal antibody blocking Fc receptor functions. II. Studies of B73.1 antibody–antigen interaction on the lymphocyte membrane. *J. Immunol.* 130:2142–2148.

Piper, J. W., R. A. Swerlick, and C. Zhu. 1998. Determining force dependence of two-dimensional receptor–ligand binding affinity by centrifugation. *Biophys. J.* 74:492–513.

Rascu, A., R. Repp, N. A. C. Westerdaal, J. R. Kalden, and J. G. J. van de Winkel. 1997. Clinical relevance of Fcγ receptor polymorphisms. *Ann. NY Acad. Sci.* 815:282–295.

Ravetch, J. V., and B. Perussia. 1989. Alternative membrane forms of FcγRIII(CD16) on human natural killer cells and neutrophils. Cell type-specific expression of two genes that differ in single nucleotide substitutions. *J. Exp. Med.* 170:481–497.

Salmon, J. E., J. C. Edberg, and R. P. Kimberly. 1996. FcγR on neutrophils. *In* Human IgG Fc Receptors. J. G. J. van de Winkel and P. J. A. Capel, editors. R. G. Landes, Austin, TX.79–105.

Scallon, B. J., E. Scigliano, V. H. Freedman, M. C. Miedel, Y. C. Pan, J. C. Unkeless, and J. P. Kochan. 1989. A human immunoglobulin G receptor exists in both polypeptide-anchored and phosphatidylinositol-glycan-anchored forms. *Proc. Natl. Acad. Sci. USA.* 86:5079–5083.

Selvaraj, P., O. Carpen, M. L. Hibbs, and T. A. Springer. 1989. Natural killer cell and granulocyte Fcγ receptor III (CD16) differ in membrane anchor and signal transduction. *J. Immunol.* 143:3283–3288.

Selvaraj, P., W. F. Rosse, R. Silber, and T. A. Springer. 1988. The major Fc receptor in blood has a phosphatidylinositol anchor and is deficient in paroxysmal nocturnal haemoglobinuria. *Nature.* 333:565–567.

Shen, L., P. M. Guyre, and M. W. Fanger. 1987. Polymorphonuclear leukocyte function triggered through the high affinity Fc receptor for monomeric IgG. *J. Immunol.* 139:534–538.

van de Winkel, J. G. J., and P. J. A. Capel. 1996. Human IgG Fc Receptors. R. G. Landes, Austin, TX.

Warmerdam, P. A., J. G. van de Winkel, E. J. Gosselin, and P. J. Capel. 1990. Molecular basis for a polymorphism of human Fcγ receptor II (CD32.). *J. Exp. Med.* 172:19–25.

Williams, T. E., P. Selvaraj, and C. Zhu. 2000. Concurrent binding to multiple ligands: kinetic rates of CD16b for membrane-bound IgG1 and IgG2. *Biophys. J.* 79:1858–1866.

Wolfram Research. 1996. Mathematica 3.0 Standard Add-on Packages. Wolfram Media and Cambridge University Press, New York, NY.

Zhu, C., and T. E. Williams. 2000. Modeling concurrent binding of multiple molecular species in cell adhesion. *Biophys. J.* 79:1850–1857.